

Thermochemical behaviour of Algal Waste: Kinetics and Mechanism of the Pyrolysis

A. Aboulkas^{1,2*}, A. Tabbal¹, H. Bouaik¹, M. El Achaby³, K. El harfi¹, A. Barakat²

¹Laboratoire des procédés chimiques et matériaux appliqués (LPCMA), Faculté polydisciplinaire de Béni-Mellal, Université Sultan Moulay Slimane, BP 592, 23000 Béni-Mellal, Morocco.

²IATE, CIRAD, Montpellier SupAgro, INRA, Université de Montpellier, 34060, Montpellier, France.

³Materials Science and Nanoengineering Department, Mohamed 6 Polytechnic University, Lot 660-Hay MoulayRachid, 43150 Benguerir.

Abstract: The present work assesses a possible process for treating algal wastes in an environmentally friendly way. It is based on the pyrolysis of these wastes for energetic valorization in order to evaluate its bioenergy potential. The pyrolytic and kinetic characteristics of algal waste as a model for algal biomass were evaluated and compared at heating rates of 5, 10, 20 and 50 °C min⁻¹ from 105 to 900 °C in an inert atmosphere. The DTG curves showed three distinct stages of degradation; dehydration, devolatilization and residual decomposition. The kinetic analysis was established by the isoconversional methods of Friedman (FR), Flynn-Wall-Ozawa (FWO) and Vyazovkin (VYA) methods to estimate activation energy, the master-plot methods were introduced to establish kinetic models. Activation energy values were shown to be 192.55, 183.26 and 185.45 kJ mol⁻¹ as calculated by FR, FWO and VYA methods, respectively. The devolatilization stage of algal waste could be described by the Avramic-Erofeev equation (n = 3). It is shown that the isoconversional kinetic methods provide the reliable kinetic information suitable for adequately choosing the kinetic model which best describes the thermal decomposition of algal waste. The composite differential method was used to obtain the following kinetic triplet: $f(x) = [3(1-x)^{2/3}]/[2(1-(1-x)^{1/3})]$, $E_a = 191.67 \text{ kJ mol}^{-1}$, $A = 1.16 \times 10^{15} \text{ min}^{-1}$

Keywords: Algal waste; thermal degradation; Isoconversional methods; master-plots method; Kinetic triplet.

1. Introduction

The energy demand and climate change has led the world to discover new secure energy sources that are renewable, environment-friendly, affordable and above all sustainable. The limited reserve of fossil fuel and increase in energy consumption force us to research in alternative and renewable energy sources [1]. Due to its abundance, renewability and higher energy density, biomass is considered as the most promising alternative-energy source to fuel the future of mankind [2]. As a consequence there is interest in alternative biomass resources including biomass from an aquatic environment. Marine macroalgae is one such source of aquatic biomass and potentially represents a significant source of renewable energy in coming years. The average photosynthetic efficiency of aquatic biomass is 6-8% [3], which is much higher than terrestrial biomass ones (1.8-2.2%).

The marine areas of Morocco include almost 3500 km of coastline [4]. The macroalgae are considered economically valuable resources due to their ability to produce high yields of commercially valuable biomass [5]. The abundance of the *Gelidium sesquipedale* macroalgae encourages the development of the industrial units specialized in the production of the agar-agar, whose Morocco is the third producer in the world [6]. The *Gelidium* represents 90% of the harvest of the marine algae treated

locally and that generates an important quantity of waste that cannot be treated very well [7]. The wastes from their processing also represent as a feedstock to make renewable fuels. The valorization of algal waste via thermochemical conversion technologies, and more specifically *via* pyrolysis appears to be notably interesting. During pyrolysis a significant amount of biofuel (bio-oil, bio-char and bio-gas) is produced [8,9]. It could be used as biofuel if its quality is appropriate. In addition, the pyrolytic gas can be used as a combustible fuel, while the char has various applications including fertilizer, activated carbon material and carbon sequestration [10].

For the proper design and operation of the pyrolysis conversion systems, a thorough knowledge of the thermal behaviour and pyrolysis kinetics of biomass are required. Thermogravimetric analysis (TGA) was selected for the thermal decomposition process [11-13]. The kinetic data obtained from TGA are very useful in helping us understand the thermal degradation processes and mechanisms; these data also may be used as input parameters for a thermal degradation reaction model [14,15]. Many studies have been published on the pyrolysis characteristics and kinetics of macroalgae [16-20]. Anastasakis et al. [16] performed a pyrolysis behavior study of the main carbohydrates of brown macroalgae, and Py-GC/MS results showed that each of the model compounds produced a

characteristic fingerprint. TGA analysis has revealed the different degradation pathways of the carbohydrates. Laminarin and alginic acid were found to have lower activation energies than mannitol and fucoidan. Activation energy for fucoidan was high for biomass samples (247.2 kJ/mol). Kim et al. [17] investigated the pyrolysis characteristics and kinetics of *Alga Sagarssum* sp. Biomass using a thermogravimetric analyzer and tubing reactor. The global kinetic parameters of *Sagarssum* sp. including the apparent activation energies were determined by differential methods. The activation energies of the pyrolysis of *Sagarssum* sp. were between 183.53 and 525.57 kJ/mol. *Sagarssum* sp. bio-oil showed the highest selectivity for dianhydro-mannitol when pyrolysis was carried out at 380 °C for 4 min in a micro-tubing reactor. Li et al. [18] studied the pyrolytic and kinetic characteristics of three kinds of red algae at heating rates of 10, 30 and 50 C min⁻¹ under an inert atmosphere. The Popescu, FWO and KAS methods were adopted to determine the kinetic parameters of the reaction. During the primary decomposition reactions, the three macroalgae species exhibited the reaction mechanism of random nucleation followed by growth (n = 3). The activation energy calculated by these three methods is similar. However, there are no reports in the literature on the Kinetics and mechanism of the pyrolysis of algal waste from the Agar-Agar industry.

Algal waste offer a low cost biomass for bioenergy production but its thermal conversion into energy requires to understand its pyrolytic characteristics and kinetics. Aiming at this, the present study was focused on the thermal characterization of this low-cost biomass, for the very first time, using thermogravimetric analysis. The kinetic parameters were determined by the isoconversional (integral and differential methods) and the kinetic model was determined by the integral and differential master plots methods. Finally, for checking the correctness of determined reaction model (f(α)), the direct differential method was applied.

2 Experimental

2.1 Materials and samples preparation

Algal waste used in this study as a feedstock was obtained from the industrial processing of red macroalgae to obtain Agar product (SETEXAM company, Kenitra-Morocco). Prior to use, algal waste was air-dried, ground and sieved to obtain particles in the ranges of 0.1-0.2 mm. The chemical compositions of samples are depicted in Table 1.

Table 1. Main characteristics of algal waste.

Proximate analysis (wt.%)	Moisture	5.04
	Volatile matter	68.91
	Ash	12.09

	Fixed carbon	19.00
Ultimate analysis (wt.%)	C	35.27
	H	4.71
	N	4.44
	S	0.73
	O	54.85
HHV (MJ/kg)		14.98
Atomic	H/C	1.60
	O/C	1.17
Empirical formula		CH _{1.603} O _{1.166} N _{0.108}

2.2 Experimental Techniques

Algal waste sample was subjected to thermogravimetric analysis (TGA) in an inert atmosphere of nitrogen. METTLER TOLEDO (TGA/DSC 3+) was used to measure and record the sample mass change with temperature over the course of the pyrolysis reaction. Thermogravimetric curves were obtained at four different heating rates (5, 10, 20 and 50°C min⁻¹) between 105°C and 900°C. Nitrogen gas was used as an inert purge gas to displace air in the pyrolysis zone, thus avoiding unwanted oxidation of the sample. A flow rate of around 60 ml min⁻¹ was fed to the system from a point below the sample and a purge time of 60 min (to be sure the air was eliminated from the system and the atmosphere is inert). The balance can hold a maximum of 45 mg; therefore, all sample amounts used in this study averaged approximately 20 mg. The reproducibility of the experiments is acceptable and the experimental data presented in this paper corresponding to the different operating conditions are the mean values of runs carried out two or three times.

3. Kinetic modeling

The mass loss curves obtained at constant heating rate were transformed into the conversion (x) versus temperature curves by means of the following equation:

$$x = \frac{w_0 - w}{w - w_f} \quad (1)$$

where w is the weight of the sample at a given time t , w_0 and w_f , refer to values at the beginning and the end of the weight loss event of interest.

In kinetic analysis, it is generally assumed that the rate of heterogeneous solid-state reaction can be described by two separate functions $k(T)$ and $f(x)$ such that:

$$\frac{dx}{dt} = k(T) f(x) = A \exp\left(-\frac{E}{RT}\right) f(x)$$

$k(T)$ is a temperature-dependent constant and $f(x)$ is the reaction model, which describes the dependence of the reaction rate on the extent of reaction.

3.1 Isoconversional methods

3.1.1 Differential isoconversional method: Friedman method (FR) [21]

This method is a differential isoconversional method, and it directly based on Eq. (2) whose logarithm is

$$\ln\left(\frac{dx}{dt}\right) = \ln[Af(x)] - \frac{E}{RT} \quad (3)$$

From this equation, it is easy to obtain values for E over a wide range of conversions by plotting $\ln\left(\beta \frac{dx}{dT}\right)$ against

$$\frac{1}{T} \text{ for a constant } x \text{ value.}$$

3.1.2 Integral isoconversional method: Flynn-Wall-Ozawa method (FWO)[22–24]

The above rate expression can be transformed into non-isothermal rate expressions describing reaction rates as a function of temperature at a constant β ($\beta = dT/dt$):

$$\frac{dx}{dT} = \frac{1}{\beta} A \exp\left(-\frac{E}{RT}\right) f(x) \quad (4)$$

Integrating up to the conversion, a, Eq. (5) gives

$$g(x) = \int_0^x \frac{dx}{f(x)} = \frac{A}{\beta} \int_{T_0}^T \exp\left(-\frac{E}{RT}\right) dT \quad (5)$$

where $g(x)$ is the integral kinetic function or integral reaction model when its form is mathematically defined in Table 2.

One of the methods to obtain the E from dynamic data may be the one used by Flynn, Wall and Ozawa[22–25] using the Doyle’s approximation of $p(x)$ [26], which involves measuring the temperatures corresponding to fixed values of x from experiments at different heating rates. This is one of the integral methods that can determine the E which does not require the knowledge of reaction order.

$$\ln(\beta) = \ln\left[\frac{AE}{Rg(x)}\right] - 5.331 - 1.052 \frac{E}{RT} \quad (6)$$

Thus, for $x = const.$, the plot $\ln \beta$ vs. $\frac{1}{T}$, obtained from thermograms recorded at several heating rates, should be a straight line whose slope can be used to evaluate the activation energy.

3.1.3 Integral isoconversional method: Vyazovkin (VYA)[27]

Another isoconversional method is the one developed by Vyazovkin and Lesnikovich [28] that allows both simple and complex reactions to be evaluated[29].

In Eq. (5), since $E/2RT \gg 1$, the temperature integral can be approximated by

$$\int_{T_0}^T \exp\left(-\frac{E}{RT}\right) dT \approx \frac{R}{E} T^2 \exp\left(-\frac{E}{RT}\right) \quad (7)$$

Substituting the temperature integral and taking the

$$\ln\left(\frac{\beta}{T^2}\right) = \ln\left[\frac{RA}{Eg(x)}\right] - \frac{E}{RT}$$

For each conversion value (x), $\ln(\beta/T^2)$ plotted versus $1/T$ gives a straight line with slope $-E/R$. Thus, E is obtained as a function of the conversion.

3.2. Masterplots method

The master plots are curves of the theoretical function of the reaction model and are independent of the Arrhenius parameters. The experimental kinetic data can easily be transformed into master plots, and the comparison between the theoretical and the experimental master plot leads to the selection of the appropriate reaction model, or at least, the appropriate type of kinetic model. There are two types of master plots: differential and integral.

Using as a reference point at $x = 0.5$, the following differential master equation is easily derived from Eq. (3):

$$\frac{f(x)}{f(0.5)} = \frac{dx/dt}{(dx/dt)_{0.5}} \frac{\exp(E/RT)}{\exp(E/RT_{0.5})} \quad (9)$$

where $(dx/dt)_{0.5}$, $T_{0.5}$ and $f(0.5)$ are respectively the reaction rate, the temperature reaction and the differential conversion function at $x = 0.5$. The theoretical curves are obtained by plotting $\frac{f(x)}{f(0.5)}$ against x for different reaction models. The resulting experimental

$$\frac{dx/dt}{(dx/dt)_{0.5}} \frac{\exp(E/RT)}{\exp(E/RT_{0.5})}$$

values are plotted against x and

matched with the theoretical masterplots.

Using as reference point at $x = 0.5$, the following integral master equation is easily derived from Eq. (5):

$$\frac{g(x)}{g(0.5)} = \frac{p(x)}{p(x_{0.5})} \quad (10)$$

where $p(x_{0.5})$ is the temperature integral at $x = 0.5$; $p(x)$ has been obtained according to the Senum-Yang approximation[29]:

$$p(x) = \frac{e^{-x}}{x} \frac{x^3 + 18x^2 + 86x + 96}{x^4 + 20x^3 + 120x^2 + 240x + 120} \quad (11)$$

Using the integral Coats-Redfern method based on Eq. (8)[30,31], the Eq. (10) becomes:

$$\frac{g(x)}{g(0.5)} = \frac{T^2}{T_{0.5}^2} \frac{\exp(-E/RT)}{\exp(-E/RT_{0.5})} \quad (12)$$

The theoretical curves are obtained by plotting $\frac{g(x)}{g(0.5)}$ against x for different reaction models. The resulting experimental $\frac{T^2}{T_{0.5}^2} \frac{\exp(-E/RT)}{\exp(-E/RT_{0.5})}$ values are plotted against x and matched with the theoretical masterplots.

All plots were generated and the lines were fitted using the origin 9.1 software (OriginLab Corporation)

Table 2. Set of reaction models applied to describe the reaction kinetics in heterogeneous solid state systems.

Model		Differential form	Integral form
		$f(x) = \frac{1}{k} \frac{dx}{dt}$	$g(x)$
Nucleation models			
Power law	P2	$2x^{1/2}$	$x^{1/2}$
Power law	P3	$3x^{2/3}$	$x^{1/3}$
Power law	P4	$4x^{3/4}$	$x^{1/4}$
Avarami-Erofeyev	A2	$2(1-x)[- \ln(1-x)]^{1/2}$	$[- \ln(1-x)]^{1/2}$
Avarami-Erofeyev	A3	$3(1-x)[- \ln(1-x)]^{2/3}$	$[- \ln(1-x)]^{1/3}$
Avarami-Erofeyev	A4	$4(1-x)[- \ln(1-x)]^{3/4}$	$[- \ln(1-x)]^{1/4}$
Geometrical contraction models			
Contracting area	R2	$2(1-x)^{1/2}$	$[1 - (1-x)^{1/2}]$
Contracting volume	R3	$3(1-x)^{2/3}$	$[1 - (1-x)^{1/3}]$
Diffusion models			
1-D diffusion	D1	$1/2x$	x^2
2-D diffusion	D2	$[- \ln(1-x)]^{-1}$	$[(1-x) \ln(1-x)] + x$
3-D diffusion, Jander	D3	$3(1-x)^{2/3} / [2(1-(1-x)^{1/3})]$	$[1 - (1-x)^{1/3}]^2$
Ginstling-Brounshtein	D4	$3/[2((1-x)^{-1/3} - 1)]$	$1 - (2x/3) - (1-x)^{2/3}$
Reaction-order models			
First-order	F1	$(1-x)$	$- \ln(1-x)$
Second-order	F2	$(1-x)^2$	$(1-x)^{-1} - 1$
Third-order	F3	$(1-x)^3$	$[(1-x)^{-2} - 1]/2$

4. Results and Discussion

4.1 Thermogravimetric analysis

The results of thermogravimetric experiments on algal waste were expressed in terms of the conversion x . The conversion versus temperature at heating rates of 5, 10, 20, and 50 C/min for algal waste obtained via TGA are shown in Fig. 1. The TGA and DTG graphs reveal three different stages in the thermal decomposition of the algal waste. The first stage occurred in the temperature range from 213 to 407 °C, the second stage was from 407 to 600 °C, and the third stage was from 600 to nearly 800 °C. The first and second stages represent the main devolatilization, during which most of the algal waste weight was lost due to the degradation of volatile components. In the first stage, the DTG curves exhibited one visible peak that reached its maximum value between 333 and 360 °C. This stage represents the decomposition of the carbohydrate and the protein content. Considering the previous studies regarding the TGA experiments with several types of proteins and carbohydrates [16,32], it can be said that

overlap may exist between thermal degradation temperatures of proteins and carbohydrates in this temperature range. During the second stage, the carbon-containing compounds in the solid residues continuously decomposed at a very slow rate. A slight continued loss of weight is shown in the weight loss curve. In the second stage, TGA-pyrolysis shows a gradual loss in mass above 500 °C which can be attributed to volatile metal loss and carbonate decomposition [8,33,34]. A significant proportion of inorganic materials in kelps decompose at 600 - 800 °C, probably a consequence of mineral components in the algal waste [8,33,35,36]. Ferrera-Lorenzo et al. [8] analyzed Pyrolysis characteristics of a macroalgae solid waste and found two distinguishable peaks during the devolatilization stage. They attributed the first peak at 315-350 °C to degradation of carbohydrates and proteins and the second peak at 480 °C to the decomposition of volatile metal. Ross et al. [33] investigated the pyrolysis behavior of five macroalgae, finding that the carbohydrates and proteins decomposed between 180 and 450 °C. These

differences in decomposition temperatures were attributed to the different compositions of the macroalgae; in particular, the chemical compositions and structures can vary both from species to species and in response to differences in conditions [16,34,37].

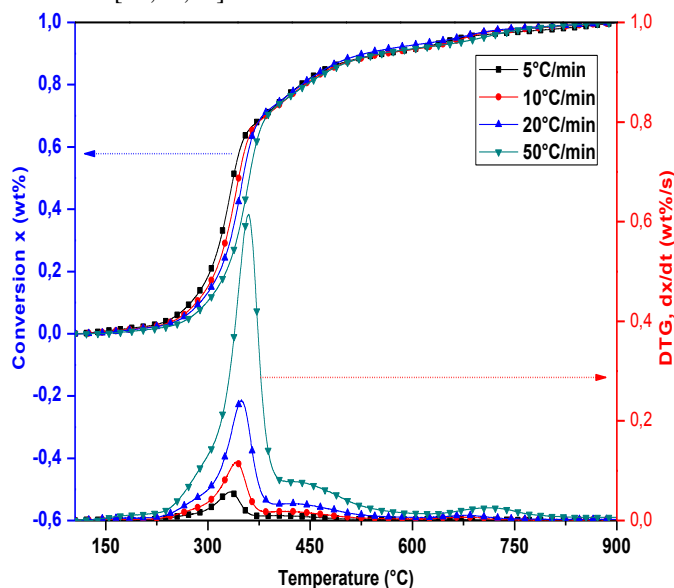


Figure 1. The TG and DTG curves of algal waste at different heating rates.

The effect of heating rate is shown in Fig. 1. Heating rate affects TG curve positions, maximum rate of decomposition and location of maximum T_m peaks. The maximum rate of dx/dt in the DTG curves increased with increasing heating rate. The maximum rate of decomposition tended to increase at higher heating rates because there was more thermal energy, which facilitated the transfer of heat between the surroundings and the interiors of the samples [8,13,16,34,38]. The maximum point rates of decomposition observed in the DTG curves occurred at 333, 342, 350 and 360 °C at heating rates of 5, 10, 20, and 50 °C/min, respectively.

4.2 Kinetic analysis

Different temperature ranges should be chosen at different heating rates during the second stage. Then, the conversion rate can be calculated corresponding to the chosen temperature scope, especially the conversion rate here is calculated during the main reaction interval which begins at the lowest temperature and terminates at the highest temperature of all heating rates. The results obtained from thermogravimetric analysis were utilized to calculate the activation energy E_a according to the differential and integral isoconversional methods. In this study, Friedman, FWO, and Vyazovkin methods were adopted to elaborate the data. Firstly, the isoconversional Friedman method was employed to calculate activation energy from a plot of $\ln(dx/dt)$. Friedman linear fit of a plot of $\ln(dx/dt)$ against $\frac{1}{T}$ for algal waste thermal degradation process is shown in Table 3. The value of the activation energy E_a was 192.55 ± 7 kJ mol⁻¹ derived from the slope of such

regression line being $-E_a/RT$. Activation energies corresponding to the different conversion x , have been also calculated using FWO and VYA methods according to Eqs. (6) and (8). The FWO plots of at progressing conversion values, with the slope of such line being $-1.052 \frac{E_a}{RT}$, are displayed in Table 3. The Vyazovkin plots of $\ln(\beta/T^2)$ versus $1/T$ at progressing conversion values, with the slope of such line being $-E_a/RT$, are depicted in Table 4. The mean activation energies calculated from FWO and VYA methods were 183.26 ± 3 and 185.45 ± 7 kJ mol⁻¹, respectively. The dependence of apparent activation energy (E_a) on the degree of conversion (x) (E_a - x curve) for non-isothermal decomposition process of algal waste obtained by isoconversional methods is presented in Fig. 2. From this figure, one can notice the same shapes of the curves E_a versus x corresponding to the considered isoconversional methods. Also, it can be seen that the values of apparent activation energy (E_a) calculated by FWO and VYA integral methods are lower than values of E_a calculated by FR differential method. The differences observed can be assigned to the different approximations. It can be observed that the calculated average values of apparent activation energy for FWO and VYA methods are very similar.

Table 3. Activation energy of algal waste by FWO, VYA and FR.

Conversion degree/ x	Activation energy E_a (Kj/mol)		
	FWO	VYA	FR
0.1	183.8	189.7	192.2
0.15	178.7	189.6	196.5
0.2	179.3	195.3	180.3
0.25	180	176.1	189.6
0.3	180.8	175.9	194.5
0.35	184.3	169.1	176.8
0.4	183.9	175	191.2
0.45	181	187.8	184.9
0.5	183.6	187.8	197.7
0.55	183.8	187	197.3
0.6	182.1	187.8	200.1
0.65	183.3	188	199.9
0.7	184.9	188.3	195.1
0.75	188.4	187.8	196.7
0.8	187.6	188.8	197.5
0.85	183.9	189.1	196.5
0.9	186.1	189.5	186.6
Average	183.26 ± 3	185.45 ± 7 187.09 ± 5	192.55 ± 7

The knowledge of x as a function of temperature and the value of the activation energy are essential in order to calculate the experimental master plot against x from experimental data obtained under a linear heating rate (Eq. (9) and (12)). Fig. 3 shows the experimental master plots against x constructed from experimental data under

different heating rates using the 187.09 kJ mol⁻¹ mean activation energy obtained the FWO, VYA and FR methods. The theoretical master plots corresponding to the $g(x)$ functions in Table 2 are also shown in Fig. 3. It is shown that the all experimental master plots of decomposition process at 5, 10, 20 and 50 °C min⁻¹ are consistent with theoretical masterplot for D3 kinetic model. The comparison of the experimental masterplots with theoretical ones revealed that the kinetic process for the decomposition process of algal waste was most probably described by the 3-D diffusion, Jander (D3) model, $g(x) = [1 - (1 - x)^{1/3}]^2$. To confirm the kinetic model the reaction follows, the integral master plots are constructed according to eq.(9), using the activation energy (187.09 kJ mol⁻¹). The results are illustrated in Fig. 4, where the experimental master plots under different heating rates are compared with the theoretical masterplots corresponding to the $f(x)$ functions in Table 2. It is clear that the experimental master plots appear to follow 3-D diffusion, Jander (D3) model, $f(x) = [3(1 - x)^{2/3}]/[2(1 - (1 - x)^{1/3})]$.

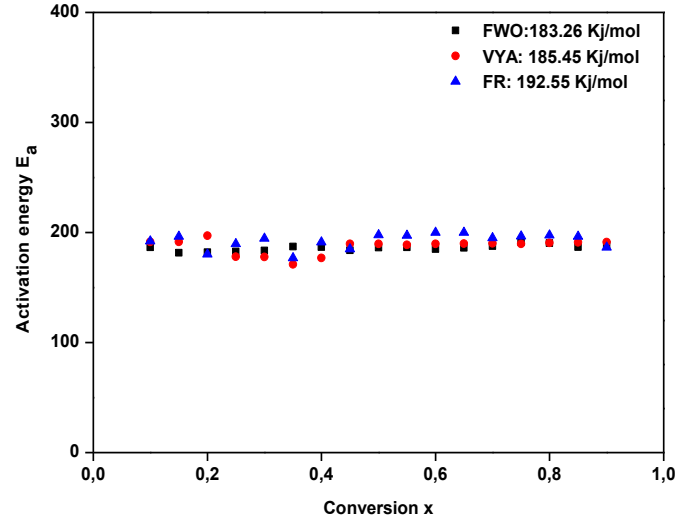


Figure 2. The dependence of activation energy (E_a) on the conversion (x) for decomposition process of algal waste according to FR, FWO and VYA isoconversional methods.

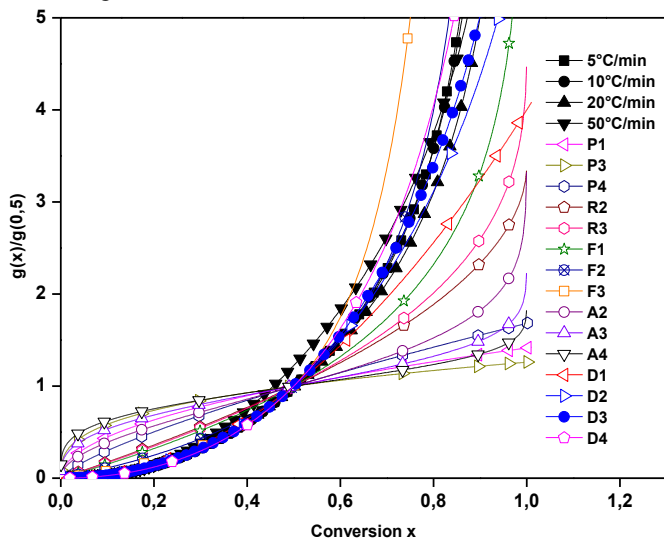


Figure 3. Theoretical integral master plots of $g(x)/g(0.5)$ vs x and the experimental master curves.

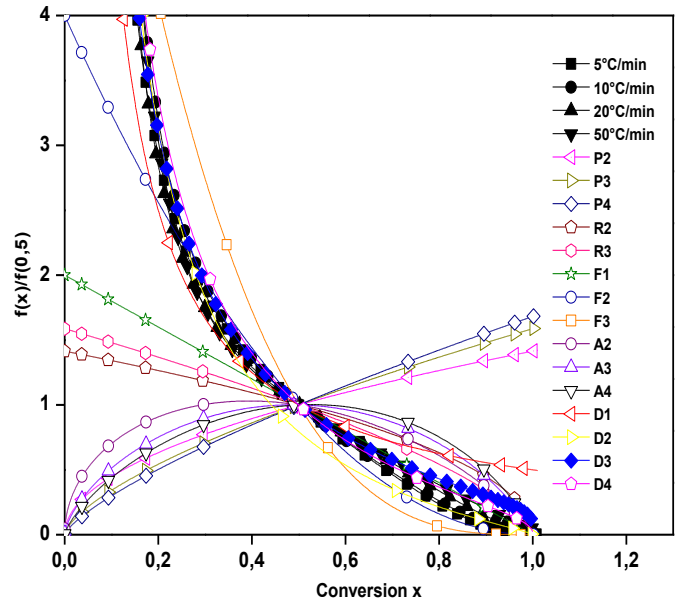


Figure 4. Theoretical differential master plots of $f(x)/f(0.5)$ vs x and the experimental master curves.

For checking the correctness of determined conversion function ($f(x)$), the equation (10) (direct differential method (D)) was used. The curves $\ln[\beta(d\alpha/dT)/f(\alpha)]$ versus $1/T$ for the $f(x)$ corresponding to D3 kinetic model, and all used heating rates were drawn. All points are placed around/on the same line only for D3 kinetic model (3-D diffusion, Jander (D3) model) (Fig. 5). From the parameters of this straight line the Arrhenius parameters were evaluated obtaining $\ln A = 34.69$ ($A = 1.16 \times 10^{15} \text{ min}^{-1}$) and $E_x = 191.67 \text{ kJ mol}^{-1}$ ($r = -0.9989$). The values of Arrhenius parameters obtained by the differential method are in good agreement with values of Arrhenius parameters obtained by FR isoconversional method.

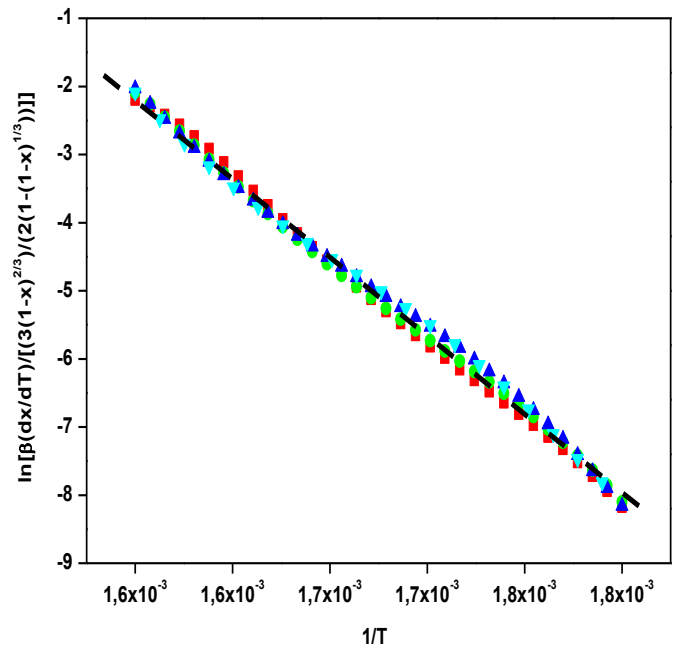


Figure 5. The straight line $\ln[\beta(dx/dT)/[3(1 - x)^{2/3}]/[2(1 - (1 - x)^{1/3})]]$ vs. $(1/T)$ for the thermal decomposition process of algal waste at all the used heating rates.

5. Conclusions

This paper explores the kinetics of algalwaste thermal degradation under a combined isoconversional and generalized masterplots approach. The activation energy for the pyrolysis was in range 183-193 kJ mol⁻¹ and it was found that a 3-D diffusion, Jander (D3) kinetic model governs the reaction. A satisfying agreement of obtained kinetic triplet curves $[f(x) = [3(1-x)^{2/3}]/[2(1-(1-x)^{1/3})]]$, $E_a = 191.67 \text{ kJ mol}^{-1}$, $A = 1.16 \times 10^{15} \text{ min}^{-1}$ with those experimentally obtained was put in evidence.

The results suggested that the experimental results and kinetic parameters provided useful information for the design of pyrolytic processing system using algal waste as feedstock. Further investigation of pyrolysis products is required to fully understand the mechanisms of thermal degradation of algal waste.

References

1. J.M. Amezaga, D.N. Bird, J.A. Hazelton, The future of bioenergy and rural development policies in Africa and Asia, *Biomass Bioenergy*. 59 (2013) 137–141. doi:10.1016/j.biombioe.2013.10.001.
2. O.K. Lee, E.Y. Lee, Sustainable production of bioethanol from renewable brown algae biomass, *Biomass Bioenergy*. 92 (2016) 70–75. doi:10.1016/j.biombioe.2016.03.038.
3. K. Miyamoto, Renewable biological systems for alternative sustainable energy production, *Food & Agriculture Org.*, 1997. https://books.google.com/books?hl=fr&lr=&id=KB1XH4IgTqkC&oi=fnd&pg=PR3&dq=Renewable+Biological+Systems+for+Alternative+Sustainable+Energy+Production&ots=LbQjJ7NuA3&sig=GW6dI-6l3SVSETh0ym_5wyLK6WU (accessed May 25, 2017).
4. T. Ainane, Valorisation de la biomasse algale du Maroc: Potentialités pharmacologiques et Applications environnementales, cas des algues brunes *Cystoseira tamariscifolia* et *Bifurcaria bifurcata*, *Faculté des Sciences Ben M'sik Université Hassan II Casablanca*, 2011. <https://hal.archives-ouvertes.fr/tel-00637002/> (accessed March 20, 2017).
5. N. Hanif, M.C. Idrissi, T. Naoki, others, L'exploitation des algues rouges *Gelidium* dans la région d'El-Jadida: aspects socio-économiques et perspectives, *Afr. Sci. Rev. Int. Sci. Technol.* 10 (2014). <http://www.ajol.info/index.php/afsci/article/view/109806> (accessed March 20, 2017).
6. A. Mouradi-Givernaud, L.A. Hassani, T. Givernaud, Y. Lemoine, O. Benharbet, Biology and agar composition of *Gelidium sesquipedale* harvested along the Atlantic coast of Morocco, *Hydrobiologia*. 398-399 (1999) 391–395.

doi:10.1023/A:1017094231494.

7. M. Ennouali, M. Ouhssine, K. Ouhssine, M. Elyachioui, Biotransformation of algal waste by biological fermentation, *Afr. J. Biotechnol.* 5 (2006). <http://www.ajol.info/index.php/ajb/article/view/43087> (accessed March 17, 2017).
8. [8] N. Ferrera-Lorenzo, E. Fuente, I. Suárez-Ruiz, R.R. Gil, B. Ruiz, Pyrolysis characteristics of a macroalgae solid waste generated by the industrial production of Agar–Agar, *J. Anal. Appl. Pyrolysis*. 105 (2014) 209–216.
9. N. Ferrera-Lorenzo, E. Fuente, J.M. Bermúdez, I. Suárez-Ruiz, B. Ruiz, Conventional and microwave pyrolysis of a macroalgae waste from the Agar–Agar industry. Prospects for bio-fuel production, *Bioresour. Technol.* 151 (2014) 199–206.
10. N. Ferrera-Lorenzo, E. Fuente, I. Suárez-Ruiz, B. Ruiz, Sustainable activated carbons of macroalgae waste from the Agar–Agar industry. Prospects as adsorbent for gas storage at high pressures, *Chem. Eng. J.* 250 (2014) 128–136.
11. K. Jayaraman, M.V. Kok, I. Gokalp, Thermogravimetric and mass spectrometric (TG-MS) analysis and kinetics of coal-biomass blends, *Renew. Energy*. 101 (2017) 293–300. doi:10.1016/j.renene.2016.08.072.
12. K. Jayaraman, M.V. Kok, I. Gokalp, Combustion properties and kinetics of different biomass samples using TG–MS technique, *J. Therm. Anal. Calorim.* 127 (2017) 1361–1370. doi:10.1007/s10973-016-6042-1.
13. M.V. Kok, E. Ozgur, Characterization of lignocellulose biomass and model compounds by thermogravimetry, *Energy Sources Part Recovery Util. Environ. Eff.* 39 (2017) 134–139. doi:10.1080/15567036.2016.1214643.
14. M.Y. Guida, H. Bouaik, A. Tabal, A. Hannioui, A. Solhy, A. Barakat, A. Aboulkas, K.E. Harfi, Thermochemical treatment of olive mill solid waste and olive mill wastewater, *J. Therm. Anal. Calorim.* 123 (2016) 1657–1666. doi:10.1007/s10973-015-5061-7.
15. M.S. Ahmad, M.A. Mehmood, O.S. Al Aayed, G. Ye, H. Luo, M. Ibrahim, U. Rashid, I. Arbi Nehdi, G. Qadir, Kinetic analyses and pyrolytic behavior of Para grass (*Urochloa mutica*) for its bioenergy potential, *Bioresour. Technol.* 224 (2017) 708–713. doi:10.1016/j.biortech.2016.10.090.
16. K. Anastasakis, A.B. Ross, J.M. Jones, Pyrolysis behaviour of the main carbohydrates of brown macro-algae, *Fuel*. 90 (2011) 598–607. doi:10.1016/j.fuel.2010.09.023.
17. S.-S. Kim, H.V. Ly, J. Kim, J.H. Choi, H.C. Woo, Thermogravimetric characteristics and pyrolysis

- kinetics of Alga *Sagarssum* sp. biomass, *Bioresour. Technol.* 139 (2013) 242–248. doi:10.1016/j.biortech.2013.03.192.
18. D. Li, L. Chen, X. Zhang, N. Ye, F. Xing, Pyrolytic characteristics and kinetic studies of three kinds of red algae, *Biomass Bioenergy.* 35 (2011) 1765–1772. doi:10.1016/j.biombioe.2011.01.011.
 19. M. Radhakumari, D.J. Prakash, B. Satyavathi, Pyrolysis characteristics and kinetics of algal biomass using tga analysis based on ICTAC recommendations, *Biomass Convers. Biorefinery.* 6 (2016) 189–195. doi:10.1007/s13399-015-0173-7.
 20. K. Wu, J. Liu, Y. Wu, Y. Chen, Q. Li, X. Xiao, M. Yang, Pyrolysis characteristics and kinetics of aquatic biomass using thermogravimetric analyzer, *Bioresour. Technol.* 163 (2014) 18–25. doi:10.1016/j.biortech.2014.03.162.
 21. H.L. Friedman, Kinetics of thermal degradation of char-forming plastics from thermogravimetry. Application to a phenolic plastic, *J. Polym. Sci. Part C Polym. Symp.* 6 (1964) 183–195. doi:10.1002/polc.5070060121.
 22. J.H. Flynn, L.A. Wall, A quick, direct method for the determination of activation energy from thermogravimetric data, *J. Polym. Sci. [B].* 4 (1966) 323–328.
 23. J.H. Flynn, L.A. Wall, General treatment of the thermogravimetry of polymers, *J Res Nat Bur Stand.* 70 (1966) 487–523.
 24. T. Ozawa, A New Method of Analyzing Thermogravimetric Data, *Bull. Chem. Soc. Jpn.* 38 (1965) 1881–1886.
 25. T. Ozawa, Kinetic analysis of derivative curves in thermal analysis, *J. Therm. Anal. Calorim.* 2 (1970) 301–324.
 26. C.D. Doyle, Kinetic analysis of thermogravimetric data, *J. Appl. Polym. Sci.* 5 (1961) 285–292.
 27. S. Vyazovkin, A.I. Lesnikovick, Transformation of “degree of conversion against temperature” into “degree of conversion against time” kinetic data, *Russ J Phys Chem.* 62 (1988) 1535–1537.
 28. S. Vyazovkin, N. Sbirrazzuoli, Confidence intervals for the activation energy estimated by few experiments, *Anal. Chim. Acta.* 355 (1997) 175–180.
 29. G.I. Senum, R.T. Yang, Rational approximations of the integral of the Arrhenius function, *J. Therm. Anal.* 11 (1977) 445–447.
 30. A.W. Coats, J.P. Redfern, Kinetic Parameters from Thermogravimetric Data, *Nature.* 201 (1964) 68–69. doi:10.1038/201068a0.
 31. A.W. Coats, J.P. Redfern, Kinetic parameters from thermogravimetric data. II., *J. Polym. Sci. [B].* 3 (1965) 917–920. doi:10.1002/pol.1965.110031106.
 32. B. Maddi, S. Viamajala, S. Varanasi, Comparative study of pyrolysis of algal biomass from natural lake blooms with lignocellulosic biomass, *Bioresour. Technol.* 102 (2011) 11018–11026. doi:10.1016/j.biortech.2011.09.055.
 33. A.B. Ross, J.M. Jones, M.L. Kubacki, T. Bridgeman, Classification of macroalgae as fuel and its thermochemical behaviour, *Bioresour. Technol.* 99 (2008) 6494–6504.
 34. J. Yanik, R. Stahl, N. Troeger, A. Sinag, Pyrolysis of algal biomass, *J. Anal. Appl. Pyrolysis.* 103 (2013) 134–141. doi:10.1016/j.jaap.2012.08.016.